G Model
CULHER-2698; No. of Pages 7

ARTICLE IN PRESS

Journal of Cultural Heritage xxx (2013) xxx–xxx

Available online at
SciVerse ScienceDirect
www.sciencedirect.com

Elsevier Masson France
EM|consulte
www.em-consulte.com/en

Case study

# Multi-image 3D reconstruction data evaluation

Anestis Koutsoudis[a,*], Blaž Vidmar[b], George Ioannakis[a], Fotis Arnaoutoglou[a], George Pavlidis[a], Christodoulos Chamzas[c]

[a] Institute for Language and Speech Processing, Multimedia Department, Research Centre "Athena", PO BOX 159, 67100 Xanthi, Greece
[b] University of Ljubljana, Faculty of Civil and Geodetic engineering, 1000 Ljubljana, Slovenia
[c] Democritus University of Thrace, Faculty of Electrical and Computer Engineering, 67100 Xanthi, Greece

ARTICLE INFO

*Article history:*
Received 9 October 2012
Accepted 10 December 2012
Available online xxx

*Keywords:*
3D range scanning
Structure-From-Motion
Dense multi-view 3D reconstruction
Total station survey
3D data comparison
Unmanned aerial vehicle

ABSTRACT

A number of software solutions based on the Structure-From-Motion (SFM) and Dense Multi-View 3D Reconstruction (DMVR) algorithms have been made recently available. They allow the production of high quality 3D models by using unordered image collections that depict a scene or an object from different viewpoints. In this work, we question the quality of the data produced by a commercial SFM-DMVR software. An Ottoman monument located in the region of Xanthi, Greece has been selected as a case study. We attempted to quantify the quality of the SFM-DMVR data in relation to the data produced by a Time-of-Flight terrestrial 3D range scanner. We have implemented a number of comparisons between different parts of the monument in order to assess the mesh deviations and the reconstruction's accuracy. In order to further ensure the validity of our evaluation phase, we performed additional distance measurements between feature points on the monument's surface by using a total station and empirical measurements. The applicability of the SFM-DMVR method was questioned by creating a complete 3D digital replica of the monument.





## 1. Research aims

In this work, we are evaluating the accuracy of the data produced by a multi-image 3D reconstruction technique that is of a lower cost in terms of hardware requirements, knowledge background and man-hours when compared with 3D range scanning. For the produced data evaluation, we have performed the 3D digitisation of the same monument with other methods such as terrestrial 3D laser scanning, total station surveying and empirical measurements. We compared the data produced by each method in terms of surface deviation and distance measurements accuracy. The main aim of our research is to objectively quantify the quality of the 3D model produced by the image-based method, to evaluate the methods applicability in a real case scenario and to provide objective evaluation indicators regarding the advantages and limitations of the image-based 3D reconstruction method.

## 2. Introduction

The use of 3D content derived from the cultural heritage domain has dramatically increased over the last decade. At present, a number of initiatives in the form of research and development projects are focused on establishing 3D documentation as an affordable, practical and effective mechanism that allows the content enrichment of cultural heritage digital libraries with 3D digital replicas [1–3]. Nowadays, 3D digitisation is considered as a common practice in the cultural heritage domain [4]. Most of the currently available hardware solutions produce high quality results. However, they introduce an increase in project's budget not only because of the equipment involved but also because of the data processing procedures that require advanced knowledge in areas such as terrestrial surveying and 3D data processing [5,6]. A cost-effective and efficient way in terms of hardware requirements, knowledge background and man-hours for producing high quality 3D digital replicas of real world objects is always a prerequisite for a digitisation project.

In this paper, we discuss the idea of replacing a 3D range scanner with a digital camera and a commercial software solution that implements the Structure-From-Motion (SFM) and Dense Multi-View 3D Reconstruction (DMVR) algorithms. We have selected Agisoft PhotoScan [7] as one of the major commercial SFM-DMVR representatives currently available. We consider the software as an

* Corresponding author.
*E-mail addresses:* akoutsou@ceti.gr, a_koutsoudis@hotmail.com (A. Koutsoudis), blazvidmar@student.uni-lj.si (B. Vidmar), gioannakis@gmail.com (G. Ioannakis), fotarny@ceti.gr (F. Arnaoutoglou), gpavlid@ceti.gr (G. Pavlidis), chamzas@ee.duth.gr (C. Chamzas).

1296-2074/$ – see front matter © 2013 Elsevier Masson SAS. All rights reserved.
http://dx.doi.org/10.1016/j.culher.2012.12.003

all-to-one software solution for the production of digital 3D replicas of monuments. We assess the applicability of the method by creating a complete exterior 3D model of a monument using both terrestrial and aerial photography. We evaluate the quality of the resulted 3D mesh by comparing it against the data captured by other methods such as terrestrial 3D laser scanning, total station surveying and empirical measurements.

The rest of this paper is organised as follows. In Section 2, we describe some of the major SFM-DMVR software solutions that are currently available along with references to related works that also attempt to provide suggestions of the method's applicability. In Section 3, we give a historical outline of the monument and we continue by describing the digitisation procedures being followed. In Section 4, we discuss the 3D reconstruction procedure and Section 5 presents the data comparison and evaluation results. We conclude in Section 6 by outlining the important findings.

## 3. Related work

A number of software solutions, implementing the Structure-From-Motion (SFM) and Dense Multi-View 3D Reconstruction (DMVR) algorithms from image collections have been made available to the broad public over the last years. The SFM method uses a number of unordered images that depict a static scene or an object from arbitrary viewpoints and attempts to recover camera parameters and a sparse point cloud that represents the 3D geometry of a scene. The method mainly[1] uses the corresponding features, which are shared between different images that depict overlapping areas, to calculate the intrinsic and extrinsic parameters of the camera [8]. Many systems involve the bundle adjustment method in order to improve the accuracy of calculating the camera trajectory, to minimize the projection error and also to prevent the error-built up of the camera tracking [9]. Snavely et al. proposed a method that allows the exploration of images that have been organised in 3D space by using Bundler, an open source SFM system [10,11]. A similar Web-based system is being currently offered by Microsoft [12].

Furthermore, Wu et al. have recently developed a version of bundle adjustment that uses hardware parallelism [13,14]. Their software also integrates the work presented by Furukawa et al. that is able to ignore non-rigid objects (e.g. passing pedestrians) [15]. The EU funded project 3D-COFORM has implemented an SFM-DMVR system as a Web-service [16]. Comparable systems have been created by Autodesk [17], Viztu Technologies [18] and Acute3D [19].

In addition, companies offer multi-image-based 3D reconstruction solutions as standalone applications. Eos Systems Inc. offers PhotoModeler Scanner [20]. The software is able to reconstruct the content of an image collection as a 3D dense point cloud with the help of photogrammetric targets. Towards the same direction, Agisoft offers PhotoScan [7]. This software solution can merge the independent depth maps of all images and produce a single vertex painted point cloud that can be converted to a triangulated 3D mesh of different densities. Moreover, Pix4D developed the Pix4UAV software that is able to create 3D digital elevation models from image collections captured by UAVs [21].

As the popularity of such 3D reconstruction solutions is being increased, several authors are attempting to evaluate the quality of the produced data. Neitzel et al. [22] and R. Opitz et al. [23] have questioned the quality and performance of some of the above software solutions in creating 3D digital elevation models. Jeroen De Reu et al. [24] and M. Doneus et al. [25] have demonstrated the use of Agisoft PhotoScan as a cost-effective method for the recording of archaeological excavations while Nguyen et al. [26] have subjectively compared the results produced by their own SFM-DMVR system against some of the previously described systems.

## 4. 3D digitisation session of the Ottoman monument

In this section, we provide some historic information about the monument and we describe the data collection procedures that have been followed and the equipment being used.

### 4.1. *Case study: the Kioutouklou Baba Bekctashic Tekke*

The monument is located in the middle of a cultivable area on the west coast of the Vistonida lake in Xanthi, Greece. It is considered as one of the most important Ottoman monuments in the area and it may have been built in the late 15th century. It was possibly built on the ruins of an Orthodox Christian temple that was dedicated to Saint George Kalamitziotis [27], while for the Muslims it is considered as the grave of a Whirling Dervishe, named Kioutouklou Baba [28]. According to Lowry [28] the term *tekke* (gathering place for Dervishes) is erroneous as the monument is a tomb (*türbe*).

### 4.2. *Collecting data*

The fieldwork was separated into five sessions. The first two involved the terrestrial and aerial photo shooting of the monument. Then, the terrestrial 3D laser scanning session took place followed by the total station survey and the empirical measurements session.

For the terrestrial photo shooting session a DSLR Nikon D40 at 6.1 MP with an 18–55 mm lens along with a tripod have been used. On the other hand, for the aerial photo shooting session, a remote controlled helicopter has been used. The UAV was equipped with a three axis pan-tilt-roll remote controlled camera head (360° on the horizontal axis, 220° on the vertical axis and a rolling ability of 60°). A DSLR Canon EOS350d at 8.1MP with an 18–55 mm lens has been used for the aerial photo shooting session. The total number of photographs that has been used for the generation of the 3D model of the monument was 652 (469 terrestrial photos and 183 aerial photos). The average distance of the camera from the monument's surface was estimated at 4 m.

Furthermore, an Optec Ilris-$3_6$D time-of-flight range scanner has been used [29]. The system's specifications indicate a minimum distance of 3 m between the scanner and the surface to be scanned. The system offers 7 mm standard deviation error for measurements implemented at a hundred meters distance and a 2 cm maximum distance between two sequential points at a thousand meters distance. The integrated digital camera of the scanner has a 3.1 MP CCD sensor but the colour quality is considered to be poor when compared with similar systems.

A total of 24 partial scans were captured. The average distance from the monument was 16.55 m while the average distance between two consecutive points was 1.37 cm. A complete digitisation of the monument using the range scanner was not achieved. Scaffolding constructions was necessary in order to capture the top of the monument and this was out of the scope and breadth of this work. Nevertheless, the range scans covered both high and low-curvature areas that were enough for validating the quality of the data produced by PhotoScan.

In addition, a number of distinct and visibly strong feature points on the surface of the monument were selected. These points had a random spatial distribution on the surface of the monument. A total of 33 points were measured using a Topcon GPT-3005 N total station [30].

Finally, the empirical measurements session involved the measurement of short distances between several details on the surface

[1] There are SFM methods in the literature which do not rely on the corresponding information [36].

of the monument. Again, a total of 10 distances between distinct points were captured.

## 5. 3D model generation

SFM-DMVR methods require a large amount of memory and processing power in order to solve the 3D reconstruction problem. In this work, a high-end standalone computer system has been used. The system was equipped with an 8-core Intel i7 processor at 3.50 Ghz, 32GB of RAM and a NVidia Geforce GTX580 3GB RAM graphics card running Microsoft Windows 7 64-bit. The standard edition of AgiSoft PhotoScan (Version 0.8.5) has been used.

Once the user provides the software with an image collection, the system almost automatically calibrates the cameras based on the EXIF information found in the images, aligns them into the 3D space and produces a complete and single 3D mesh using a dense multi-view reconstruction algorithm [31,32].

The software offers a number of predefined 3D reconstruction levels of detail (LOD). The level of detail affects the density of the reconstructed 3D mesh. Fig. 1 depicts the different LODs of a small part of the monument's exterior surface. On Fig. 1, the colour of the mesh is given at the vertices level (Vertex Painted Mesh) and thus the higher the LOD, the higher the colour details on the model. Nevertheless, PhotoScan can also produce textured mapped meshes by blending parts of the images so that a photorealistic result can be achieved with low complexity 3D meshes. In addition, the total time required for the software to align the images into 3D space was 26 h. Table 1 presents some of the most important properties of the different LOD reconstructed meshes. It should be noted that the computer system being used didn't succeed in creating a complete ultra-high LOD 3D mesh from the given image selection. A complete 3D reconstruction of the monument's exterior is presented on Fig. 2.

The current case study came to verify that the SFM-DMVR methods are no exception to one of the basic 3D digitisation rules. This is that the processing time of the 3D data is always much higher than the time required for the data collection. In order to reduce the 3D reconstruction processing time, manual masking of the images was carried out in order to remove areas of the sky, the foliage and the monuments surroundings. Additionally, the dimensions of the 3D model produced by the software are proportional. Hence, an appropriate affine transform (symmetrical scaling in all axes) has to be applied in order for the model to depict real world dimensions. The affine transform was automatically implemented in Meshlab during the alignment session of PhotoScan model against the range scans.

## 6. Data comparison and results evaluation

We have selected to evaluate the medium 3D reconstruction resolution offered by the software as the properties of the produced mesh are considered the closest to the specifications and abilities offered by current average cost graphics card.

A total of 11 single-view range scans were used as the ground truth data. The selection criteria for these range scans were: the practically parallel positioning of the scanner's sensor plane against the monument's large planar surfaces and the relatively low average distance between the scanner's position and the monument.

The 3D data comparison pipeline that we followed included open source software such as Meshlab [33] and CloudCompare [34]. Meshlab was used to align the partial scans of the range scanner with the 3D model produced by PhotoScan. On the other hand, the CloudCompare software was used to estimate the surface deviation between the PhotoScan data and the range scanner data. We chose to compare single-view range scans against the PhotoScan model. This resulted in more accurate surface deviation measurements between the two data types. An alignment and merging procedure of the different range scans using an algorithm such as the iterative closest point (ICP) would build-up the surface deviation error. This is due to the fact that ICP is attempting to minimise (distribute) the alignment error between all the overlapping neighbouring meshes. Nevertheless, the ICP algorithm, implemented in Meshlab, has been

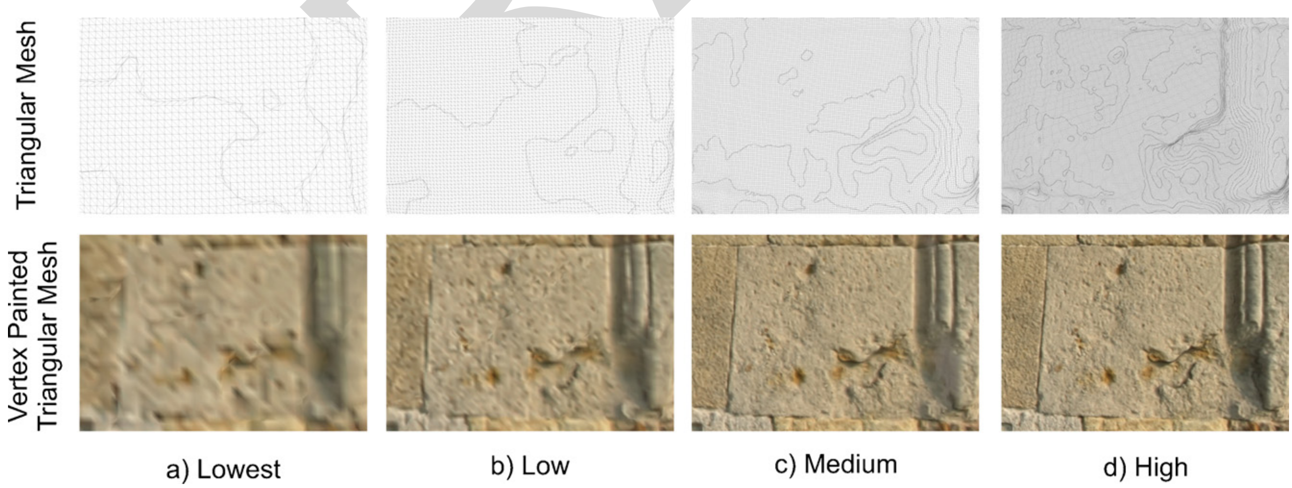


**Fig. 1.** Different LODs of the triangular mesh.

**Table 1**
PhotoScan: properties of the reconstructed mesh at different LODs.

| LOD | Number of vertices | Number of faces | Distance between vertices (mm) | Size (MB) (file format: PLY) | Total processing time (min) |
|---|---|---|---|---|---|
| Lowest | 1,567,136 | 3,049,047 | 55 | 80 | 16 |
| Low | 6,347,734 | 12,381,156 | 25 | 325 | 43 |
| Medium | 29,598,434 | 58,141,745 | 15 | 1440 | 2 h 46 |
| High | 161,537,781 | 317,769,170 | 3 | 6554 | 17 h 25 |

Please cite this article in press as: A. Koutsoudis, et al., Multi-image 3D reconstruction data evaluation, Journal of Cultural Heritage (2013), http://dx.doi.org/10.1016/j.culher.2012.12.003

used to align each single-view range scan with the PhotoScan triangular mesh model.

In order to compare the two data types, the cloud-to-mesh distance function offered by CloudCompare was selected as it is considered more robust to local noise. The cloud-to-mesh distance function computes the distances between each vertex of the point cloud to the nearest triangle of the mesh surface. The distance between the two is calculated as follow. In cases where the orthogonal projection of the vertex lies inside the surface defined by a triangle, then the distance between the vertex and its point-of-intersection on the surface is calculated. Otherwise, the software estimates the distances between the vertex and its projection to the nearest edge or to the nearest vertex of the triangle [35]. In our experiments, the PhotoScan model was always used as the mesh and each range scan as a point cloud.

Fig. 3 illustrates colour encoded surface deviations of some representative, in terms of curvature, portions of the monument's exterior surfaces. These are a north wall of the antechamber that is considered as an almost planar and of low-curvature surface, a part of the antechamber's roof tiles as a high-curvature area and a combination of both as a large portion of the monument's octagonal türbe. Each surface deviation depiction is followed by a graph showing the deviation distance frequency of occurrence along with the mean distance and the standard deviation (σ) of the three representative scans. An increase in the mean distance and the standard deviation can be seen in the part of roof tile (Fig. 3b). This is an indication of the inability of SFM-DMVR methods to reconstruct low-feature surfaces. The low frequency of colour alternations on the roof tiles in conjunction with the bad lighting in the hollow areas between every alternate roof tile row composes a challenging surface for SFM-DMVR methods.

**Table 2**
Mean distances and standard deviations of all single-view range scans compared against the PhotoScan mesh (in meters).

| Scan No. | Mean distance | Standard deviation (σ) |
|---|---|---|
| 1 | 0.001 | 0.008 |
| 2 | 0.000 | 0.005 |
| 3 | 0.003 | 0.017 |
| 4 | 0.001 | 0.010 |
| 5 | 0.001 | 0.010 |
| 6 | 0.003 | 0.020 |
| 7 | 0.004 | 0.012 |
| 8 | 0.001 | 0.006 |
| 9 | 0.003 | 0.018 |
| 10 | 0.002 | 0.013 |
| 11 | 0.002 | 0.014 |
| Weighted averages (in meters) | 0.002 | 0.014 |

In addition, Table 2 shows all the mean distances and standard deviations of the range scans that have been compared against the mesh produced by PhotoScan. It should be noted that all comparisons resulted in Gaussian like distributions. As each range scan covered an area of different size, the total number of vertices that compose each scan was used as a contribution weight to the average mean distance and standard deviation. As shown in Table 2, the total weighted average mean distance between the two data types is 2 mm and the total weighted standard deviation 14 mm.

For further assessment of the PhotoScan data, we compared a number of distance measurements between specific feature points on both data types (range scans and PhotoScan mesh) to the measurements that we have previously carried out on the actual monument using a total station. The feature points being used were apparent and easy to be recognised on the monument's surface;

**Fig. 2.** Viewpoints of the reconstructed monument (Smooth Shaded Triangular Mesh and Vertex Painted Medium Quality Triangular Mesh).

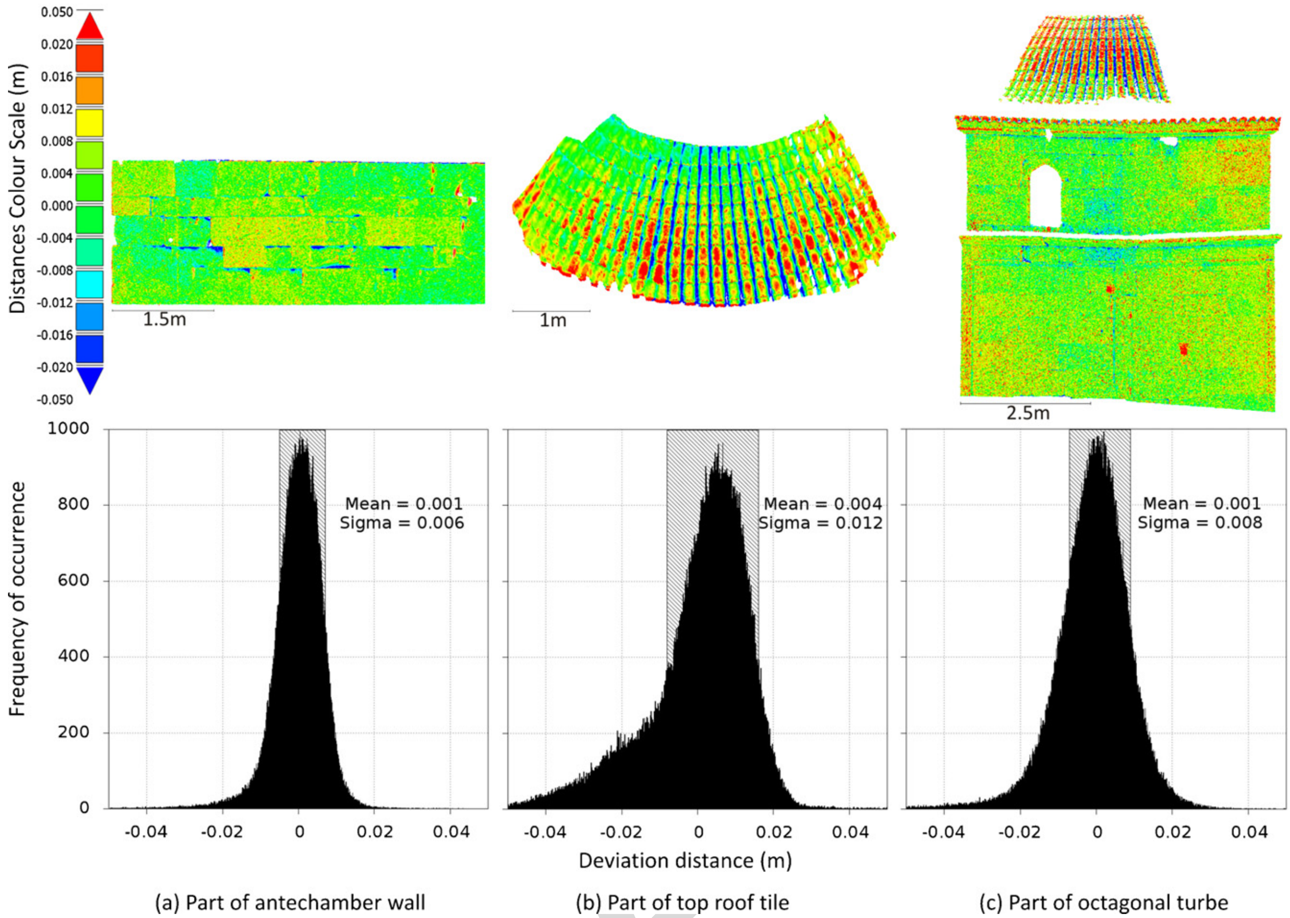


**Fig. 3.** Colour encoded surface deviation of the different parts of the monument and distance deviation distribution graphs.

Hence, their random distribution on the monument (Fig. 4). The distance differences are presented in Table 3. The manual selection of a corresponding point on the 3D data introduces an accuracy ambiguity. Nonetheless, the quality of the triangulated mesh as well as the range scanner's data provided acceptable visualisation of these features points. The average standard deviation of those Euclidean distances is around 4 mm (Table 3) while the longest distance between two feature points was 7.5 m.

On the other hand, we attempted to verify a set of empirical measurements that have been previously performed on the surface of the monument between fine details on the surface of the monument (Fig. 4). These distances varied between 7 cm and 30 cm. Again, using Meshlab, we performed the same distance measurements on the PhotoScan mesh. The results were found to be acceptable even with the ambiguity introduced by the manual selection of the corresponding points (Table 4).

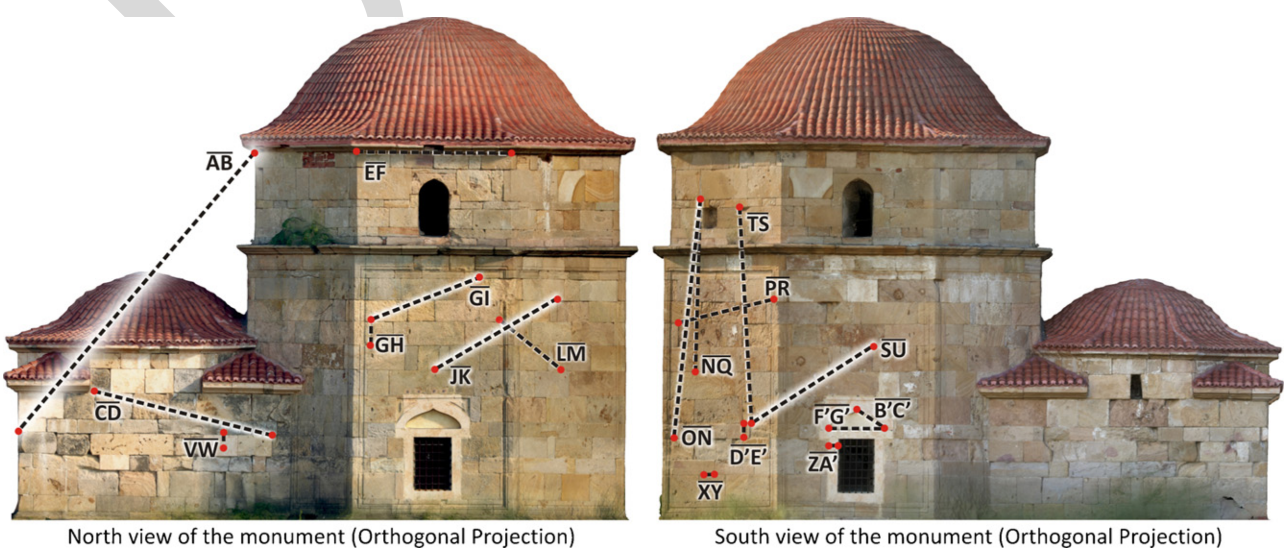


**Fig. 4.** Line segments defined by feature points on the surface of the monument used for data accuracy verification.

**Table 3**
Comparison of Euclidean distances between feature points on the different types of 3D Data (in meters).

| Line segment | Distance using total station data | Distance using range scan data | Distance using SFM-DMVR data | Standard deviation (σ) |
|---|---|---|---|---|
| $\overline{AB}$ | 7.580 | 7.592 | 7.601 | 0.008 |
| $\overline{CD}$ | 3.745 | 3.747 | 3.751 | 0.003 |
| $\overline{EF}$ | 3.184 | 3.186 | 3.189 | 0.002 |
| $\overline{GH}$ | 0.473 | 0.469 | 0.467 | 0.002 |
| $\overline{GI}$ | 2.313 | 2.313 | 2.311 | 0.001 |
| $\overline{JK}$ | 2.958 | 2.973 | 2.972 | 0.007 |
| $\overline{LM}$ | 1.876 | 1.868 | 1.881 | 0.005 |
| $\overline{NQ}$ | 3.491 | 3.496 | 3.486 | 0.004 |
| $\overline{ON}$ | 4.877 | 4.874 | 4.871 | 0.003 |
| $\overline{PR}$ | 2.661 | 2.672 | 2.665 | 0.004 |
| $\overline{SU}$ | 3.184 | 3.184 | 3.172 | 0.006 |
| $\overline{TS}$ | 4.713 | 4.703 | 4.694 | 0.008 |
| Average (in meters) | | | | 0.004 |

**Table 4**
Comparison of Euclidean distances between empirical measurements on the real monument and on the PhotoScan data.

| Line segment | Distance on real monument | Distance on SFM-DMVR data | Standard deviation (σ) |
|---|---|---|---|
| $\overline{VW}$ | 0.233 | 0.233 | 0.0000 |
| $\overline{XY}$ | 0.290 | 0.288 | 0.0010 |
| $\overline{D'E'}$ | 0.283 | 0.283 | 0.0000 |
| $\overline{ZA'}$ | 0.181 | 0.179 | 0.0010 |
| $\overline{B'C'}$ | 0.714 | 0.715 | 0.0004 |
| $\overline{F'G'}$ | 1.160 | 1.160 | 0.0001 |
| Average (in meters) | | | 0.004 |

The previous experiments contributed on verifying that the SFM-DMVR model does not contain proportional errors. SFM-DMVR methods fail to reconstruct areas of low frequency colour changes and areas that lack of strong features. Nevertheless, the results on such challenging areas can always be improved by taking pictures from a closer distance. In our case this wasn't possible due to the size of the UAV and the safety flying distance from the monument. Moving around the monument with a camera is considered efficient in relation to a range scanner but again a reduction in the efficiency factor of the method should be considered in terms of number of images against the surface area being covered.

## 7. Conclusions

In this work, we have attempted to evaluate the quality of the data produced by a 3D reconstruction commercial software that is based on the Structure-from-Motion and Dense Multi-View 3D Reconstruction algorithms. The data evaluation phase indicated that for monuments with feature-rich surfaces under appropriate lighting conditions and with the hardware and software solutions being used in this case study, high quality results can be achieved by a large set of images. A high performance computer system in terms of available memory, processing power and graphics card capabilities is a prerequisite. The produced data clearly indicate that the used hardware and software solutions can provide high quality results. But as it is an image-based technique, the produced data are highly correlated and depended on the unavoidable procedure of identifying corresponding points between images. In addition, the quality of the produced 3D model depicts the applicability of the SFM-DMVR methods in low budget digitisation or documentation projects. The semi-automated functionality of the software composes an efficient solution that also expects a low knowledge overhead from the user. Concluding, it is for certain that each technology has its advantages and disadvantages. Thus, the different 3D acquisition technologies should always be considered as supplemental. Both 3D range scanners and image-based solutions can find their applications in the cultural heritage domain. 3D range scanners have already proven their great potential on acquiring high quality 3D data from complex structures in a fast and efficient way. Nevertheless, the incorporation of 3D range scanning along with topography and photogrammetry always lead to more accurate surveys.

## Acknowledgements

This work is partially supported by the 3D-ICONS pilot project that is funded under the European Commission's ICT Policy Support Programme. The authors would like to thank Mr. Vasilis Liakopoulos and AeroView (http://www.aeroview.gr) for performing the aerial photo shooting session and Mr. Eleftherios Bourazanis for providing the total station.

## References

[1] CARARE Best Practise Network, http://www.carare.eu
[2] 3D-ICONS pilot project http://3dicons-project.eu
[3] 3D-COFORM. consortium http://3dcoform.eu
[4] A. Koutsoudis, K. Stavroglou, G. Pavlidis, C. Chamzas, 3DSSE–A 3D scene search engine: exploring 3D scenes using keywords, J Cult Heritage 13 (2012) 187–194.
[5] G. Pavlidis, A. Koutsoudis, F. Arnaoutoglou, V. Tsioukas, C. Chamzas, Methods for 3D digitisation of cultural heritage, J Cult Heritage 8 (2007) 93–98.
[6] D. Lo Buglio, L. De Luca, Critical review of 3D digitisation methods and techniques applied in the field of architectural heritage: Methodological and cognitive issues, Proceedings of the International Symposium on Virtual Reality, Archaeology and Intelligent Cultural Heritage, Prato, Tuscany, Italy, October 18–21, 2011, pp. 5–12.
[7] PhotoScan Agisoft, http://www.agisoft.ru
[8] D.P. Robertson, R. Cipolla, Structure from motion, in: Practical image processing and computer vision, John Willey and Sons Ltd, 2009.
[9] C. Engels, H. Stewénius, D. Nistér, Bundle adjustement rules, Proceedings of the photogrammetric computer vision conference, ISPRS, Bonn, Germany, September 20–22, 2006.
[10] N. Snavely, S.M. Seitz, R. Szelinski, Photo tourism: exploring image collections in 3D, Proceedings of SIGGRAPH 2006, Boston Massachusetts, July 30–August 3, USA, 2006.
[11] N. Snavely, Bundler: structure from motion for unordered image collections, http://phototour.cs.washington.edu/bundler/#S4
[12] Microsoft Photosynth http://photosynth.net
[13] C. Wu, S. Agarwal, B. Curless, S.M. Seitz, Multicore bundle adjustment, Proceedings of 24th Conference on computer vision and pattern recognition, June 20–25 Colorado Springs, 2011.

[14] C. Wu, VisualSFM: a visual structure from motion system, http://www.cs.washington.edu/homes/ccwu/vsfm, 2011.
[15] Y. Furukawa, J. Ponce, Accurate, dense and robust multi-view stereopsis, IEEE Trans. on Pattern, Anal Mach Intel 32 (2010) 1362–1376.
[16] M. Vergauwen, L. Van Gool, Web-based 3D reconstruction service, Mach Vision Appl 17 (2006) 411–426.
[17] [123D] Catch, Autodesk, http://www.123dapp.com/catch
[18] Hypr3D, Viztu Techonologies http://www.hypr3d.com
[19] Smart3DCapture, Acute3D http://www.acute3d.com/smart3dcapture
[20] PhotoModeler Scanner, http://www.photomodeler.com/products/pm-scanner.htm
[21] Pix4UAV, http://pix4d.com
[22] F. Neitzel, J. Klonowski, S. Siebert, J.P. Deshbach, Mobile 3D mapping with a low-cost UAV system on example of a landfill survey, Allgemeine Vermessungs-nachrichten AVN, Wichmann VDE-Verlag - Berlin–Offenbach (10) 2011.
[23] R. Opitz, K. Simon, A. Barnes, K. Fisher, L. Lippiello, Close-range photogrammetry vs. 3D scanning: comparing data capture, processing and model generation in the field and the lab, Proceedings of the computer applications and quantitative methods in archaeology (CAA), Avenue Campus, University of Southhampton, England, March 26–29, 2012.
[24] J. Reu, G. Plets, G. Verhoeven, P. Smedt, M. Bats, B. Cherrette, W. Maeyer, J. Deconynck, D. Herremans, P. Laloo, M. Meirvenne, W. Clercq, Towards a three-dimensional cost-effective registration of the archaeological heritage, J Archaeol Sci (2012), http://dx.doi.org/10.1016/j.jas.2012.08.040.
[25] M. Doneus, G. Verhoeven, M. Fera, Ch. Briese, M. Kucera, W. Neubauer, From deposit to point cloud – a study of low-cost computer vision approaches for the straightforward documentation of archaeological excavations, Proceedings of 23rd International CIPA Symposium, Prague, Czech Republic, September 12–16, 2011.
[26] M.H. Nguyen, B. Wuensche, P. Delmas, C. Lutteroth, 3D models from the black box: investigating the current state of image-based modeling, Proceedings of the 20th international conference on computer graphics, visualisation and computer vision (WSCG 2012), Pilsen, Czech Republic, June 25–28, 2012.
[27] G. Tsigaras, Kioutouklou Baba Bekctashic Tekke, http://www.xanthi.ilsp.gr/cultureportalweb/print.php?article_id=140&lang=en&print_mode=article
[28] H.W. Lowry, In the footsteps of the Ottomans: a search for sacred spaces and architectural monuments in northern Greece, Mary Martin Booksellers, Bahçesehir University Publications, 2009.
[29] Optech Ilris-$3_6$D time-of-flight range scanner, http://www.optech.ca/prodilris.htm
[30] Topcon GPT-3005 N total station, http://www.topcon.com.sg/survey/gpt30.html
[31] S.M. Seitz, B. Curless, J. Diebel, D. Scharstein, R. Szeliski, Evaluation of multi-view stereo reconstruction algorithms, Proceedings of IEEE computer vision and pattern recognition conference, Vol. 1 (1), Washington DC June 17–22, 2006, pp. 519–528.
[32] D. Scharstein, R. Szeliski, A taxonomy and evaluation of dense two-stereo correspondence algorithms, J Comput Vision 47 (2002) 7–42.
[33] Meshlab http://meshlab.sourceforge.net
[34] CloudCompare, http://www.danielgm.net/cc
[35] D. Eberly, Distance between point and triangle in 3D, Geometric Tools LLC, http://www.geometrictools.com/Documentation/DistancePoint3Triangle3.pdf
[36] F. Dellaert, Structure from motion without correspondence, Proceedings of the computer vision and pattern recognition, Hilton Head, South Carolina, USA, June 13–15, 2000, pp. 557–564.



Please cite this article in press as: A. Koutsoudis, et al., Multi-image 3D reconstruction data evaluation, Journal of Cultural Heritage (2013), http://dx.doi.org/10.1016/j.culher.2012.12.003